Proceedings of the 19th IAHR-APD Congress 2014, Hanoi, Vietnam

ISBN 978604821338-1

ESTIMATE OF TURBULENT FLUXES WITH EDDY—COVARIANCE TECHNIQUE IN A COMPLEX TOPOGRAPHY: A CASE STUDY IN THE ITALIAN ALPS

M. FALOCCHI(1), S. BARONTINI(1), M. TOMIROTTI(1) & R. RANZI(1)

(1) *Department of Civil, Environmental, Architectural Engineering and Mathematics, Università degli Studi di Brescia, Brescia, Italy, e-mail marco.falocchi@gmail.com, stafano.barontini@unibs.it, roberto.ranzi@unibs.it*

ABSTRACT

A sensitivity analysis to different eddy—covariance data processing algorithms is presented for a dataset collected in an Alpine environment with complex topography. In Summer 2012 a micrometeorological station was installed at Cividate Camuno (274 m a.s.l., Oglio river basin, Central Italian Alps), in a flat and rectangular grass-covered lawn. The grass was 0.6 m tall during most of the field campaign. The station is equipped with traditional devices, four multiplexed TDR probes, and an eddy--covariance apparatus sampling at 20 Hz (Gill WindMaster Sonic Anemometer and Licor Li7500 Gas Analyzer), at about 3 m above the ground. The local winds regime is strongly affected by the morphology of the valley, and the topography is complex also due to the heterogeneity of the surrounding-areas land—cover. Using EddyPro software, the sensitivity of the turbulent fluxes estimate was assessed addressing three major issues of the data processing procedure, i.e. the choice of the computational averaging period, of the axis rotation method and of the data detrending criterion. Once identified three test periods of consecutive days without rainfall, the fluxes of momentum, sensible heat and latent heat were computed at the averaging period of 30, 60 and 120 min respectively. At each averaging period, both the triple rotation method, the double rotation method and the planar fit method were applied. Particularly the latter was applied both fitting a unique plane for all the wind directions and fitting multiple planes, one for each sector of the wind rose. Regarding the detrending criteria, data were processed with a block average and a linear detrend, the latter with time constant of 5, 30, 60 and 120 min respectively. Therefore, for each test period about 50 estimates of the fluxes were provided. As a result the obtained fluxes were compared. Even if with different flux quality, their pattern is quite stable with regard to the applied estimate procedures, but with sensitively different average values.

Keywords: eddy–covariance, complex terrain, Italian Alps, CividatEX Experiment

1. INTRODUCTION

The measure of the turbulent fluxes of momentum, sensible and latent heat by means of the eddy—covariance instrumentations are useful to directly estimate the heat and moisture exchanged at the interface between ground and atmosphere.

One of the first attempts to measure the vertical fluxes exchanged at the interface between the ground and the atmosphere due to the eddy movement can be found in the work of Swinbank (1951). The aim of this work was to provide a response to the need of a direct method to measure the vertical evapotranspirative fluxes in the atmospheric surface—layer. From these experiences the formalization of the eddy—covariance technique was possible. Being developed in the framework of the classical atmospheric boundary—layer studies, *e.g.* on the works of Monin and Obukhov (1954) about the similarity theory and of Kaimal et al. (1972) about the shape of the surface—layer turbulence spectra, also the theoretical background of the eddy—covariance technique was based on the hypothesis of: (*i*) flat, horizontally homogeneous surface; (*ii*) wind speed one-dimensional along the direction of the mean wind and parallel to the ground; (*iii*) steady condition of the mean flow, (*iv*) homogeneous and fully developed turbulence. Particularly (*i*) and (*ii*) allow the vanishing of both the time—average of the vertical wind speed and the cross—correlation between the wind components, (*iii*) and (*iv*) allow to apply the ergodic hypothesis and the Reynolds decomposition hypothesis of the turbulent motion field. According to these considerations, once identified a custom time—window, the mathematical expression of the vertical turbulent fluxes was found to be proportional to the covariance between the turbulent components of the vertical wind speed and of the ones of the variable generating the flux (see *e.g.* Kaimal and Finnigan, 1994; Lee et al., 2004b).

The conceptual simplicity of the method, mainly coupled to the measurement devices improvement (in terms of precision, accuracy and sampling—rate frequency); the computational and storages resources availability; free and open—source software to the fluxes computation, in the last decades allowed to the eddy—covariance technique to obtain a great success in many fields, between which hydrology, agronomy and air pollution studies. However its application requires particular care, from the site selection, to the data processing and analysis, especially where the site characteristics do not fulfil (in part or at all) the technique basic assumptions. Particularly assumption (*i*) is the most restrictive one, because it is strictly related to the terrain configuration of the experimental site and of the surrounding area. Therefore studies aiming at extending the eddy—covariance technique applicability, also to non simple terrains, or archetypal conditions (Rotach and Zardi, 2007), were conducted (see *e.g.* McMillen, 1988 for the fluxes estimation over a forest canopy and Geissbühler et al., 2000 for measurements over mountain slopes). In this sense, the reduction of the disturbances induced to the wind flux by the topography was provided developing

correction algorithms, to apply on the data during the computational steps of the fluxes estimation. The reliability of the estimated turbulent fluxes was traditionally entrusted to the closure of the surface energy balance. Indeed, the surface energy balance closure can be regarded to as a test, in the sense that the goodness of the estimation is inversely proportional to the magnitude of the balance residuum. However, despite of the effort provided by the correction algorithms, a lack in closure of the balance, the so called "energy—imbalance", is still present. The imbalance, when referred to the entire investigated period, can be defined as the ratio between the cumulated turbulent fluxes (sensible plus latent heat) and the cumulated available energy (net radiation reduced by the ground heat flux). Typically imbalance—values range from about 10—30%, also when measurements are performed in quite—ideal terrains. Such problem has been observed and discussed in several literature studies (*e.g.* Twine et al., 2000; Kanda et al., 2004; Cava et al., 2008; Foken, 2008; Panin and Bernhofer, 2008; Leuning et al., 2012).

Between the no—ideal terrain conditions, an emblematic case is provided by the estimations of momentum, sensible and latent heat fluxes exchange in Alpine valleys (Grossi and Falappi, 2003; Rotach and Zardi, 2007; Hiller et al. 2008), that are typically characterised by high and steep slopes, complex terrain and variable wind regime. The irregularities of the valley morphology, e.g. narrowing and bights, alluvial fans and shelf, internal watersheds and hills, and the heterogeneity of the land cover, also influenced by the presence of the human activities, contribute to the complexity of the terrain. In addiction the daily wind regime, besides of the meso—scale effects, is usually characterised by local winds alternate, to drainage conditions, by transition periods (Nadeau et al., 2013). An example of drainage current is given by the katabatic winds that usually occur during night and flow downward along both the main valley direction as along the valley slopes (Whiteman, 2000). Therefore, during the day, the development of internal boundary sub—layers can be observed (*e.g.* Rotach et al., 2008). Particularly their different mechanical properties affect the fluxes regime, and thus the EC measurements.

As stated before, the estimation of the turbulent fluxes by means of the eddy—covariance technique, hereafter EC, requires the application of a certain number of correction algorithms. In this work we focused our attention on the three issues, below briefly recalled:

1. The fluxes averaging—period, and particularly its width, must be chosen in order to guarantee the stability of the statistical high order moments (Lenschow et al. 1994) and include all the relevant low—frequency contributions to the fluxes, but it should be shorter enough to avoid the unsteady of the atmosphere. Traditionally (*e.g.* Kaimal and Finnigan, 1994), an average period of 30 min was considered a good compromise to compute the EC fluxes. However Finnigan et al. (2003) found that, especially over complex terrains, longer averaging—periods, greater than 1 hour, can be considered.
2. The detrending criterion is applied to isolating the turbulent components of the signal, used to compute the fluxes, from the unsteady and long—term contributions. These effects occur especially during the transition periods, *i.e.* during the sunrise and the sunset, and can be observed also over flat and horizontal terrains (Moncrieff et al, 2004).
3. The axis rotation method, or more correctly the axis rotation method for tilt correction, is introduced to modify the sonic anemometer coordinate system in order to nullify the average cross—stream and the time—average of the vertical wind speed component (Lee et al., 2004a; Finnigan, 2004). Indeed, besides of the case in which the vertical axis of the device is not aligned to the normal at the ground, no—null values of the time—average vertical wind component can be observed when the wind speed is not parallel to the ground surface, *i.e.* over complex terrain, or when advection phenomena occur. In the literature the main rotation methods proposed, are: the triple rotation, the double rotation and the planar fit (Wilczak et al., 2001), here listed orderly to the reliability of the estimated fluxes.

In this study we present the effects on the eddy—covariance fluxes of momentum, sensible and latent heat, when estimated combining different settings of the averaging—periods, the detrending criteria and the axis rotation method. To reach this aim data collected during Summer 2012 in the framework of the CividatEX EXperiment, in an Alpine valley characterised by complex topography, were used. After a brief description of the experiment and of the experimental area (Section 2) the procedure adopted to estimate the fluxes is presented (Section 3). Finally the analysis and the results obtained are presented and discussed (Sestion 4).

2. CASE STUDY

2.1 Experimental site and the CividatEX field campaign

The Valle Camonica (Central Italian Alps) is the main valley of the Oglio river basin. It is a glacial valley, ranging from the 187 m a.s.l. at the closure of the Lake Iseo at Sarnico, to the 3539 m a.s.l. of the Adamello massif. During Summer 2012, from 9 July to the end of September, an experimental field campaign was performed at Cividate Camuno (274 m a.s.l.), called CividatEX EXperiment, aiming at assessing the energy and the water balance at the local scale in a mountain environment, characterized by a typical Alpine sublitoranean climate (Bandini, 1931). The experimental site is a flat gentle—sloping lawn mainly covered by common grass between which short spontaneous vegetation grows, particularly alfalfa (*Medicago sativa*), wild carrot (*Daucus carota*) and yarrow (*Achillea millefolium*) . At the beginning of the experiment the grass had already reached the maturation height of about 0.6 m and it was mowed only during the first week of September. The grass grew again reaching a height of about 0.10 m at the end of the field campaign.

In the center of the lawn, which can be approximated to a rectangular 95 m long in the NE—SW direction and 70 m wide in the SE—NW direction, a micrometeorological station was installed (Figure 1). The station was equipped with traditional meteorological devices, four multiplexed TDR probes and an EC apparatus was installed. Particularly the EC apparatus was composed by a Gill WindMaster 3—Axes sonic anemometers and a Li—COR Li7500 gas analyzer, places at 3.32 m and 2.98 m respectively, from the ground and both sampling at 20 Hz.

Figure 1. The micrometeorological station installed during the CividatEX experiment (Eastward, 09 July 2012) At the top of the station the eddy—covariance apparatus can be observed.

For further information about the field campaign, the soil—hydrological properties and the preliminary results obtained, please refer to Negm et al. (2013).

Even if the lawn characteristics allow to consider it as a quite—ideal site, the morphology and the land cover of the site surrounding—area does not, and therefore the terrain can be regarded to as complex. In Figure 2 the two aerial pictures, allows observing the complexity of the valley morphology and the variability of the land cover. Particularly the experimental site (yellow area) is located on the left bank of the Valle Camonica, on an ancient alluvial shelf, 10—15 m higher than the valley floor.

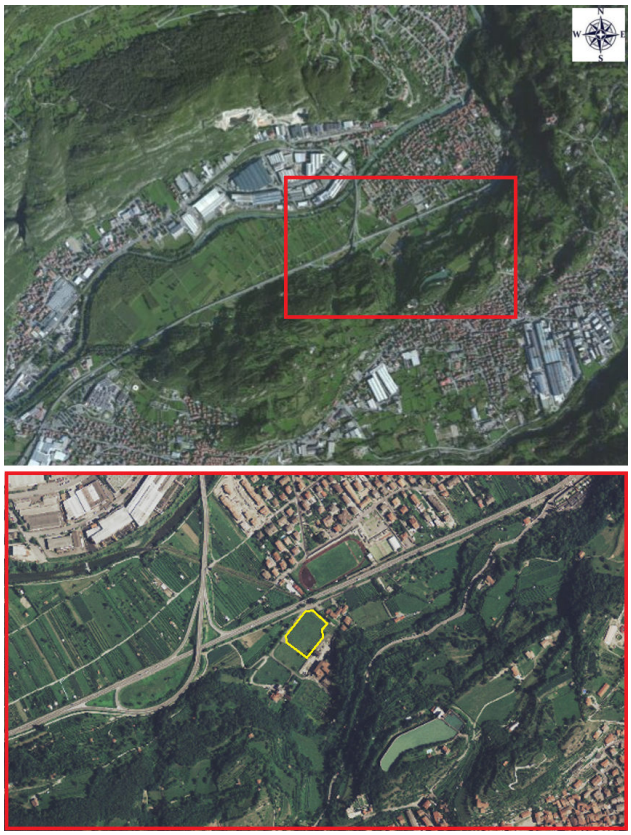

Figure 2. The Valle Camonica around the experimental site. Above the width of the valley can be detected by the presence of the valley slopes (at NW and SE). Lower, the area surrounding the experimental site (yellow) are shown.

The alluvial shelf is surrounded from E to WSW by a steep hill, which average height, of about 380 m a.s.l (E—S), decreases to 290 m a.s.l. (S—WSW), moving crosswise the main valley direction. Moreover the highly heterogeneous and different land use can be noted: at N the residential area of Cividate Camuno, at E and S to the site other buildings are present. In addition, in the area different kind of roads (from rural to highway) are present, and the variability of the green cover highlights the presence of woods and cultivated areas (mainly vineyards Westward to the site).

2.2 Local wind regime

Let us now analyze the local wind regime, by means of the wind—rose, showed in Figure 3 and obtained using the 1 min—average wind speed, recorded during the 2012 field campaign, aiming at characterize the wind regime. In the figure the pattern of the plumes and the different colors allows to identify three main wind currents and their kinematic properties.

In the Figure is evident that the most frequent drainage condition is a katabatic wind, with an average velocity ranging about 1—2 m s^{-1}, that descends the slope sited at East of the site. Indeed this wind was observed to flow from the evening to the morning. Less frequent but with higher velocities, between about 3—4 m s^{-1}, is the local wind (WSW), called *Öra*, that raises the valley from the Lake Iseo, placed about 20 km far from the site. Finally a third wind current with velocities comparable to the *Öra* ones and coming from the NNE—NE sector, was observed.

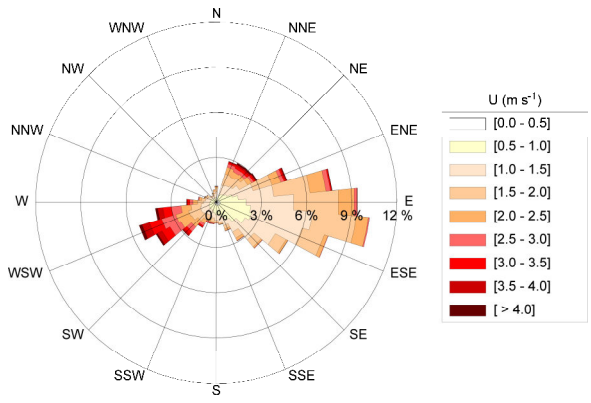

Figure 3. The local wind—rose obtained for the Summer 2012 at the experimental site, using wind data 1 minute averaged.

3. FLUXES ESTIMATION PROCEDURE

Three test periods without rain events were selected from the 2012 database: 23—28 July, 11—21 August and 20—23 September. For each period the EC fluxes were estimated using of the software EddyPro (LI—COR, 2014), with different combination and settings of the averaging—periods, rotation methods and de—trending criteria, according to the following scheme:

1. The averaging—periods (AP) of 30, 60, 120 min were chosen.
2. For each averaging period the axis rotation was performed using the triple rotation method (3R), the double rotation method (2R) and two different schemes of the planar fit method (PF1 and PF2). The PF1 was obtained fitting a unique plane for all the

wind speed directions. For the PF2, according to the wind—rose shape, six planes were fitted according to the following wind—direction sectors of width 45°, 22°.5, 45°, 112°.5, 45° and 90°, from North and rotating clockwise. To obtain the estimate of the planes the days between 8—22 August 2012 were selected and used thanks to the lack of meaningful rainfall events.

3. Finally for each rotation method the block average (BA) and the linear detrending applied as detrending criteria. The block average was used on a time window equal to the correspondent averaging period. The linear detrending, instead, was applied with four different time constants, at 5, 30, 60 and 120 min. However the cases with time constants greater than the current AP were not taken into account during the estimations.

This scheme provided a total of 48 estimates for each flux (12 for 30 min fluxes; 16 for 60 min fluxes and 20 for 120 min fluxes).

To be thorough, we list now the main unchanged settings selected for the fluxes estimation: (1) missing sample allowance at 10%; (2) time—lag compensation with covariance maximization; (3) density fluctuation compensation, according to the WPL theory (Webb et al., 1980); (4) spectral corrections according to Moncrieff et al. (2004) for low frequency range and Moncrieff et al. (1997) for the high frequency range.

4. RESULTS AND DISCUSSION

The collected realizations obtained for an AP equal to 30 and 60 minutes were further averaged over a time window of 2 hours. Moving from the homogenized databases the data analyses were performed. For each flux—type all the realizations estimated (Figure 4) and their cumulating trends (Figure 5) were analyzed.

Let us firstly consider Figure 4. Here the obtained patterns seem to be quite stable relatively to the correction algorithms considered. In other words it would appear that *a priori* the different setting of the correction algorithms produce comparable results. Such behavior is confirmed also when outsiders occurs. Indeed the heat fluxes and particularly the sensible heat one, present realizations with systematic outsiders that underestimate the flux, above all in the early evening.

In Figure 5, the integration of the fluxes of momentum, sensible heat and latent heat allowed to obtain the represented trends. In all the three patterns it was possible to recognize the daily cycle which is much more emphasized for the flux of sensible heat. The global patterns are anyway different. In fact the ensembles of the fluxes of momentum and sensible heat spans continuously a range of variability which variation coefficients are about 0.095 and 0.111 respectively with respect to the integrated average of all the realizations, that is of about 78939 kg $s^{-1}m^{-2}$ for the momentum flux and 7.04 MJ m^{-2} for the sensible heat flux. Therefore it is not possible to recognize at first sight different families of realizations. The cumulated curves of the latent heat fluxes shows instead a clearly bimodal distribution, corresponding to the families of realizations characterized by the planar fit methods (greater values) and the rotation methods (smaller values), respectively. In this case the variation coefficient of the ensemble of all the realizations with respect to an integrated average of about 161 MJ m^{-2} assumes the value of 0.08.

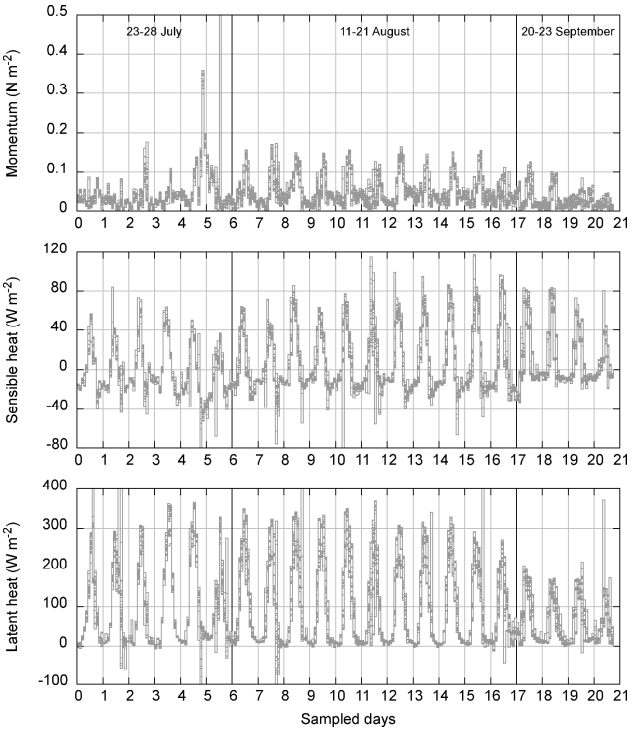

Figure 4. Realizations estimated for the fluxes of momentum, sensible and latent heat, which average are about 0.04 N m^{-2}, 4 W m^{-2} and 90 W m^{-2} respectively.

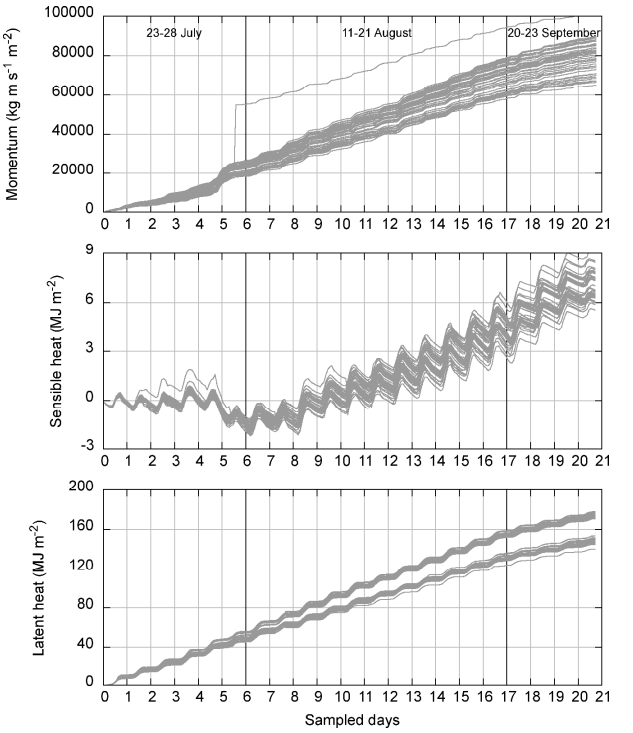

Figure 5. Integrals of the fluxes of momentum, sensible heat and latent heat.

Furthermore it is worth noting that the cumulated curves of the sensible heat flux shows almost null averages for the investigated days during July. This pattern denotes a period in which no sensible heat is accumulated in the atmosphere and in the ground below the sensor. The structure of the database allowed evidencing that at each time—step 48 estimates of the same flux were available. Therefore after estimating the average value of these 48

fluxes and the correspondent standard deviation, the bias, defined as the distance, or the fluctuation, of the flux from the corresponding average, were analyzed. In addition three averages were estimated assembling the fluxes estimated with the same AP (*i.e.* 30, 60 and 120 min). In Figure 6 the biases (points) and the ensemble averages are presented.

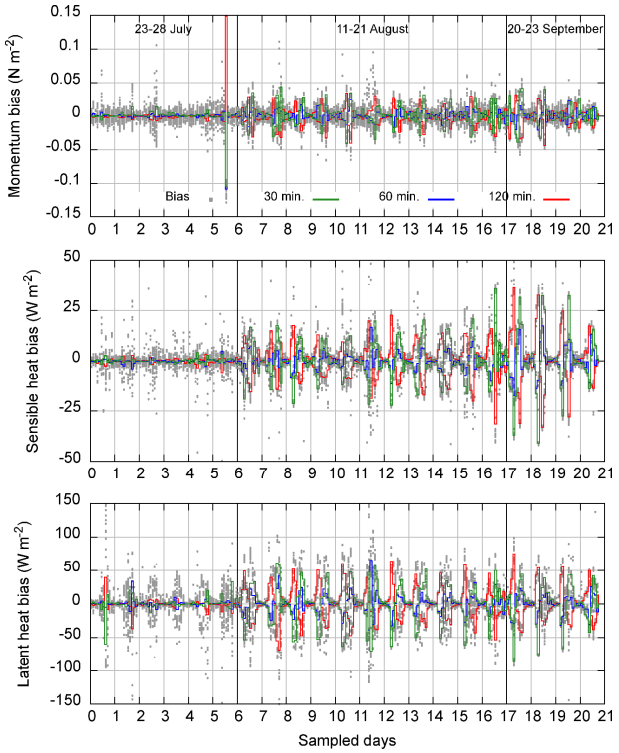

Figure 6. Bias of the fluxes from the average and ensemble average for fluxes at 30, 60 and 120 minutes.

From the Figure it can be observed that the biases fluctuate around the zero, determining a daily pattern, which was also previously observed in Figure 5. However it is remarkable the fact that for the days selected during July, the ensemble averages assume values closer to zero independently by the AP adopted to estimate the fluxes. During the remaining period, on the contrary, the ensemble averages denote a non—zero expectation associated to a phase—opposition, between of the ensemble average of 120 minutes and the ones at 30 or 60 minutes. Particularly can be noted that the 120 minutes ensemble averages, in the morning, are greater than the 30 and 60 minutes ensembles ones and, *vice versa*, in the late afternoon the 120 minutes ensemble averages are lower than the 30 and 60 minutes ensembles ones. A method to verify the existence of families of correction algorithms and settings that produce similar fluxes estimations consists to verify if the average of different data—ensembles is meaningfully different from the average of the whole ensemble. Thus we proceeded normalizing each bias by the standard deviation estimated for the correspondent time—step. The obtained normalized or dimensionless biases, hereafter pointed out with:

$$z = \frac{x - \mu}{\sigma},$$

allows to obtain a new database characterized by a null expectation and a unit standard deviation for each time—step.

In Figure 7 the normalized realizations are presented. As done in Figure 6, also here the averages of the ensembles correspondent to the AP at 30, 60 and 120 minutes are reported. In all the three patterns it is recognized that the dimensionless bias fluctuations are almost contained into the range $\pm 2\sigma$ even if outsiders are still presents, especially for the days of July. Also in this case, the ensemble averages assumes a value close to zero during July, whereas on the remaining days the averages are considerably different from zero. Moreover, as previously, the phase—opposition between the ensemble averages of the fluxes at 120 minutes with the ones at 30 and 60 minutes can be detected. Then the 48 realizations were aggregated in different ensemble and the averages were tested to check whether they were meaningfully different from zero (*e.g.* Bendat and Piersol, 1966; Kottegoda and Rosso, 1997). The confidence intervals of the null hypothesis were estimated in correspondence to the three level of significance $\alpha = 0.01$, $\alpha = 0.05$ and $\alpha = 0.10$. The test was applied on the dimensionless fluxes of momentum, sensible and latent heat, grouped according to the following criteria:

1. Fluxes estimated with the same AP (30, 60 and 120 minutes);
2. Fluxes estimated with respect to the detrending criterion: (*i*) all the block averages (BA) and (*ii*) all the linear detrending (LD);
3. Fluxes estimated with respect to the rotation method for tilt corrections: (*i*) double and triple rotations together (R); (*ii*) two planar fits method settings (PF); (*iii*) separately all the double rotations (2R), all the triple rotations (3R), all the planar fits with an unique plane (PF1) and the planar fits based on the wind—rose shape (PF2).

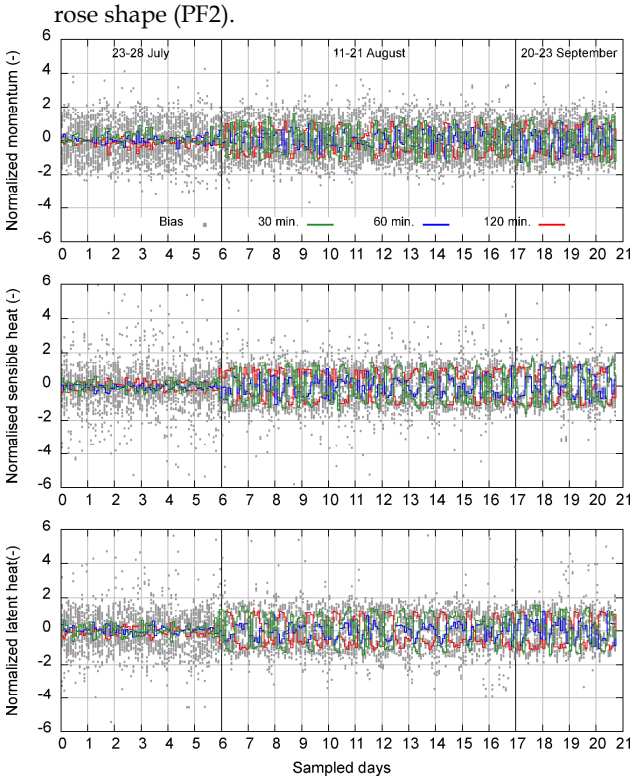

Figure 7. Normalized fluxes and ensemble average for fluxes at 30, 60 and 120 minutes.

The results obtained, reported in Table 1, show that the hypothesis of null average is rejected for most of the considered ensembles. An exception is the case of the

ensembles of 60 minutes and the two of the detrending criteria (BA and LD), for the sensible and the latent heat.

Table 1. Test on the hypothesis of a null expected value of different ensembles (if × the hypothesis is rejected at α significance, ✓ otherwise).

	Momentum			Sensible heat			Latent heat		
α	0.01	0.05	0.10	0.01	0.05	0.10	0.01	0.05	0.10
Averaging period									
30	×	×	×	×	×	×	×	×	×
60	×	×	×	✓	✓	✓	✓	✓	✓
120	×	×	×	×	×	×	×	×	×
De−trending criterion									
BA	×	×	×	✓	✓	✓	✓	✓	×
LD	✓	×	×	✓	✓	✓	✓	✓	✓
Rotation method									
R	×	×	×	×	×	×	×	×	×
PF	×	×	×	×	×	×	×	×	×
2R	×	×	×	×	×	×	×	×	×
3R	×	×	×	✓	✓	×	×	×	×
PF1	×	×	×	×	×	×	×	×	×
PF2	×	×	×	×	×	×	×	×	×

The rejection of the hypothesis of null average means that the averages of the ensembles are significantly non−zero and the ensembles belong to different families. Thus, even if at first sight the estimated fluxes, presented in Figure 4, seem to be uniform, actually they tend to assume statistically different expectations.

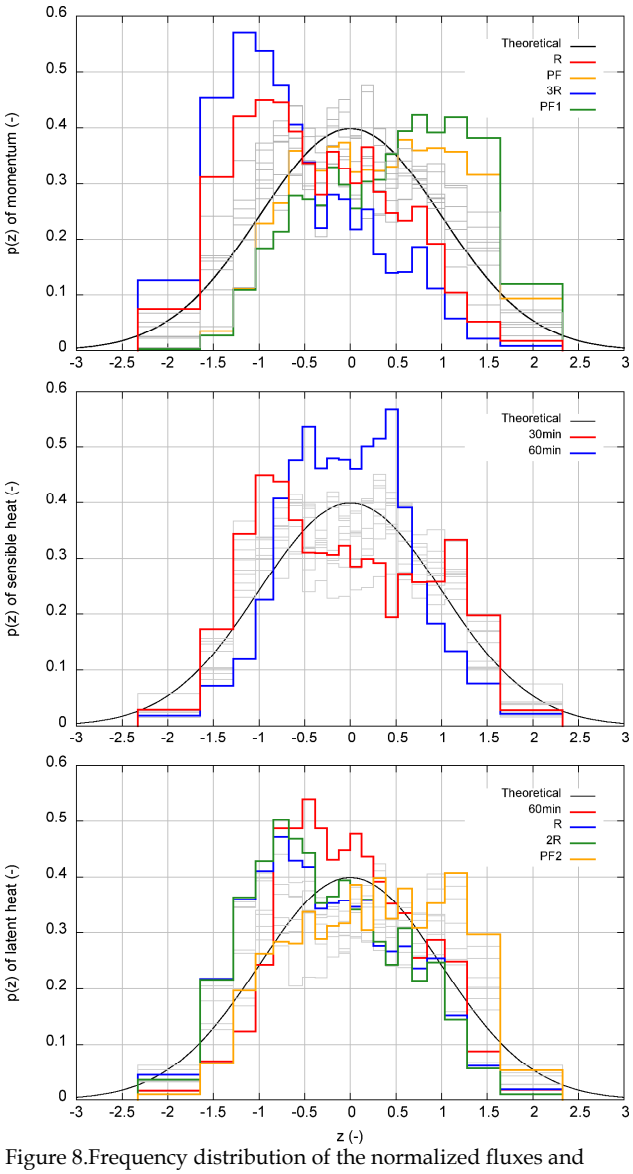

Figure 8.Frequency distribution of the normalized fluxes and comparison with the Standardized Normal Density Function.

Table 2. Asymmetry of the empirical distributions

	γ	Freq$[z \le -1.96]$	Freq$[z > 1.96]$	Freq$[\lvert z\rvert < 1]$
Standardized Normal Density Function				
	0	0.25	0.25	0.682
Momentum				
Averaging period				
30	-0.056	0.012	0.019	0.628
60	0.258	0.004	0.015	0.739
120	0.337	0.014	0.019	0.597
De−trending criterion				
BA	0.188	0.028	0.044	0.575
LD	0.152	0.004	0.011	0.677
Rotation method				
R	0.574	0.020	0.011	0.640
PF	0.014	0.001	0.025	0.665
2R	0.445	0.004	0.015	0.739
3R	0.897	0.036	0.007	0.540
PF1	-0.242	0.001	0.026	0.614
PF2	0.269	0.000	0.023	0.715
Sensible heat				
Averaging period				
30	0.117	0.009	0.006	0.626
60	0.036	0.010	0.011	0.836
120	-0.032	0.027	0.036	0.613
De−trending criterion				
BA	0.065	0.060	0.072	0.543
LD	0.021	0.002	0.004	0.739
Rotation method				
R	-0.048	0.018	0.028	0.682
PF	0.103	0.015	0.012	0.698
2R	0.116	0.013	0.031	0.691
3R	-0.195	0.024	0.025	0.673
PF1	0.086	0.014	0.011	0.702
PF2	0.122	0.016	0.012	0.694
Latent heat				
Averaging period				
30	0.415	0.016	0.020	0.603
60	0.485	0.006	0.010	0.801
120	0.242	0.017	0.013	0.620
De−trending criterion				
BA	0.497	0.042	0.032	0.595
LD	0.245	0.004	0.009	0.703
Rotation method				
R	0.828	0.020	0.016	0.689
PF	-0.033	0.007	0.012	0.664
2R	0.136	0.016	0.005	0.712
3R	1.125	0.023	0.026	0.667
PF1	-0.067	0.007	0.011	0.682
PF2	-0.005	0.006	0.013	0.646

Aiming at obtaining information about how the normalized fluxes are distributed, the frequency analysis of the 11 ensembles account for was performed.

Each frequency distribution was obtained over a set of 20 classes of probability equal to the 5%. In Figure 8 the empirical frequency distribution of each ensemble is reported. In the Figure 8 the normalized biases were pointed out with z , accordingly to the notation previously introduced and the correspondent frequency by means of $p(z)$. Moreover, besides of the Standardized Normal Density Function (black line) regarded to as a reference framework, the most relevant detected patterns are here highlighted. From the Figure 8 it can be observed that the empirical distributions show, for some realizations, patterns that are strongly different from the normal one. Particularly such patterns are characterised by a marked asymmetry that sometime is at the left−side of the Normal and sometimes at its right−side, as it is well marked in the plot of the momentum flux. Moreover, also when these distributions seem to be quite symmetric, their peaks are higher than the reference one, as in the case of

the ensembles of 60 minutes in both the sensible and in the latent heat.

Further information on the asymmetry and on the extreme distribution for the considered ensembles can be found in Table 2. The Table collects: (*i*) the skewness index (γ), (*ii*) the frequency of the values exceeding $z = \pm 1.96$ and (*iii*) the frequency of normalized values when they fall within the interval $-1 < z \leq 1$. Particularly the second point allows deriving information about the distribution of the extremes of the empirical frequencies.

We found that the highest asymmetry (in absolute value) is observed to the triple rotation ensemble in all the type of fluxes considered. Particularly the asymmetry coefficients of the sensible heat are closer to the normality than the ones of the momentum and sensible heat, as it can be recognized also in Figure 8, where the empirical distributions of the sensible heat seem to be more centered than for the ones other fluxes.

The extremes of the distributions are more symmetric respect to the interval of $|z| > 1.96$, for the fluxes of sensible and latent heat. The momentum fluxes, instead, the asymmetry coefficients are more emphasized.

Finally we found that the frequencies falling within in the interval $|z| < 1$ are almost comparable with the theoretical probability.

5. CONCLUSIONS

In this study 48 realizations of eddy—covariance fluxes of momentum, sensible and latent heat, estimated with different settings of averaging—periods (30, 60 and 120 minutes), rotation methods (double rotation, triple rotation and two setting of planar fit method) and de—trending criteria (block average and linear detrending), were statistically analyzed. The data used to the estimations were collected in the framework of the CividatEX Experiment, in an Alpine valley characterized by complex terrain and variable wind regime. Particularly a set of 21 days distributed during Summer 2012 was investigated.

The results obtained show that when eddy—covariance fluxes are estimated in such environments the choice of the set of corrections to implement plays an important role at affecting the values of the estimates. This is evident if we consider the variation coefficient of the ensemble of the fluxes, from which it emerges that the ensemble spans a meaningfully wide range of values. However if a sub—set of realizations is performed, exploring the effect of different settings of the code, the average was found to be significantly different from that of the whole ensemble, thus recognizing that different sub—sets of realizations are not able to reproduce the variability of the whole ensemble. Anyway the average values of the sub—sets, even if statistically different from the ensemble average, can be regarded to as an attempt to estimate the average of the whole ensemble. Therefore, even if further analyses are still required, also to identify the corrections that split the ensembles into two families, as it is the case of the latent heat fluxes, it is possible to reduce the uncertainty associated to the estimations, even if exploring a reduced number of realizations.

ACKNOWLEDGMENTS

Part of the research was funded in the framework of the research project PRIN 2008 "Valutazione delle risorse idriche e loro gestione in scenari di cambiamento climatico" coordinated by Prof. La Loggia, which is kindly acknowledged.

REFERENCES

Bandini A. (1931). *Tipi pluviometrici dominanti sulle regioni italiane*, Tech. report, Roma: Ministero dei Lavori Pubblici.

Bendat JS., and Piersol AG. (1966). *Measurement and Analysis of Random Data*. John Wiley & Sons.

Cava D., Contini D., Donateo A., and Martano P. (2008). Analysis of short-term closure of the surface energy balance above short vegetation. *Agricultural and forest meteorology*, 148 (1), 82-93.

Finnigan JJ., Clement R., Malhi Y., Leuning R., and Cleugh HA. (2003). A re-evaluation of long-term flux measurement techniques part I: averaging and coordinate rotation. *Boundary—Layer Meteorology*, 107 (1), 1-48.

Finnigan JJ. (2004). A re-evaluation of long-term flux measurement techniques part II: coordinate systems. *Boundary—Layer Meteorology*, 113, 1-41.

Foken T. (2008). The energy balance closure problem: An overview. *Ecological Applications*, 18 (6), 1351—1367.

Geissbühler P., Siegwolf R., and Eugster W. (2000). Eddy covariance measurements on mountain slopes: the advantage of surface-normal sensor orientation over a vertical set-up. *Boundary—Layer Meteorology*, 96 (3), 371—392.

Grossi G., and Falappi L. (2003). Comparison of energy fluxes at the land surface-atmosphere interface in an Alpine valley as simulated with different models. *Hydrology and Earth System Sciences Discussions*, 7 (6), 920—936.

Hiller R., Zeeman MJ., and Eugster W. (2008). Eddy-covariance flux measurements in the complex terrain of an Alpine valley in Switzerland. *Boundary—layer meteorology*, 127(3), 449—467.

Kaimal JC., and Finnigan JJ. (1994). *Atmospheric boundary layer flows: their structure and measurement*. Oxford University Press.

Kaimal JC., Wyngaard J., Izumi Y., and Coté, OR. (1972). Spectral characteristics of surface—layer turbulence. *Quarterly Journal of the Royal Meteorological Society*, 98, 563—589.

Kanda M., Inagaki A., Letzel MO., Raasch S., and Watanabe T. (2004). LES study of the energy imbalance problem with eddy covariance fluxes. *Boundary—Layer Meteorology*, 110 (3), 381—404.

Kottegoda NT., and Rosso R. (1997). *Statistics, probability, and reliability for civil and environmental engineers* (Vol. 735). New York: McGraw-Hill.

Lee X., Finnigan J. and Paw UKT, (2004a). Coordinate systems and flux bias error. In *Handbook of Micrometeorology* (pp. 33—66). Atmospheric and Oceanographic Sciences Library (Vol. 29). Kluwer Academic Publishers.

Lee X., Massman WJ., and Law BE. (Eds.). (2004b). *Handbook of micrometeorology: a guide for surface flux measurement and analysis*. Atmospheric and Oceanographic Sciences Library (Vol. 29). Kluwer Academic Publishers.

Lenschow DH., Mann J., and Kristensen L. (1994). How long is long enough when measuring fluxes and other

turbulence statistics?. *Journal of Atmospheric and Oceanic Technology*, 11 (3), 661—673.
Leuning R., Van Gorsel E., Massman WJ., and Isaac PR. (2012). Reflections on the surface energy imbalance problem. *Agricultural and Forest Meteorology*, 156, 65—74.
LI—COR. (2014) *EddyPro 5.0 Eddy Covariance Software, Instruction Manual*. 6th ed.
Moncrieff JB., Massheder JM., De Bruin H., Elbers J., Friborg T., Heusinkveld B., Kabat P., Scott S., Soegaard H., and Verhoef A. (1997). A system to measure surface fluxes of momentum, sensible heat, water vapour and carbon dioxide. *Journal of Hydrology*, 188, 589—611.
Moncrieff J., Clement R., Finnigan J., and Meyers T. (2004). Averaging, detrending, and filtering of eddy covariance time series. In *Handbook of micrometeorology: a guide for surface flux measurement and analysis* (pp. 7—31). Atmospheric and Oceanographic Sciences Library (Vol. 29). Kluwer Academic Publishers.
Monin AS. and Obukhov AM. (1954) Basic laws of turbulent mixing in the ground layer of the atmosphere. *Trudy Geofizicheskogo Instituta Akademiya Nauk USSR*, 151, 163—187.
McMillen RT. (1988). An eddy correlation technique with extended applicability to non—simple terrain. *Boundary—Layer Meteorology*, 43 (3), 231—245.
Nadeau DF., Pardyjak ER., Higgins CW., Huwald H. and Parlange MB. (2013). Flow during the evening transition over steep Alpine slopes. *Quarterly Journal of the Royal Meteorological Society*, 139 (672), 607—624.
Negm A., Falocchi M., Barontini S., Ranzi R. and Baldassare B. (2013). Assessment of the Water Balance in an Alpine Climate: Setup of a Micrometeorological Station and Preliminary Results. *Procedia Environmental Sciences,* 19, 275—284.
Panin GN. and Bernhofer C. (2008). Parametrization of turbulent fluxes over inhomogeneous landscapes. Izvestiya, *Atmospheric and Oceanic Physics*, 44 (6), 701—716.
Rotach MW., Andretta M., Calanca P., Weigel AP., and Weiss A. (2008). Boundary layer characteristics and turbulent exchange mechanisms in highly complex terrain. *Acta Geophysica*, 56 (1), 194—219.
Rotach MW. and Zardi D. (2007). On the boundary—layer structure over highly complex terrain: Key findings from MAP. *Quarterly Journal of the Royal Meteorological Society*, 133, 937—948.
Swinbank WC. (1951). The measurement of vertical transfer of heat and water vapour by eddies in the lower atmosphere. *Journal of Meteorology*, 8 (3), 135—145.
Twine TE., Kustas WP., Norman JM., Cook DR., Houser P., Meyers TP., Prueger JH, Starks PJ. And Wesely ML. (2000). Correcting eddy—covariance flux underestimates over a grassland. *Agricultural and Forest Meteorology*, 103 (3), 279—300.
Webb EK., Pearman GI., and Leuning R. (1980). Correction of flux measurements for density effects due to heat and water vapour transfer. *Quarterly Journal of the Royal Meteorological Society*, 106 (447), 85—100.
Whiteman CD. (2000). *Mountain meteorology: fundamentals and applications* (Vol. 355). New York: Oxford University Press.
Wilczak JM., Oncley SP., and Stage SA. (2001). Sonic anemometer tilt correction algorithms. *Boundary—Layer Meteorology*, 99 (1), 127—150.